Magneto-elastic coupling in Fe-based superconductors

S.-F. Wu,[1, 2, 3, *] W.-L. Zhang,[1] V. K. Thorsmølle,[1] G. F. Chen,[2, 4] G. T. Tan,[5] P. C. Dai,[5, 6] Y. G. Shi,[2] C. Q. Jin,[2, 4]
T. Shibauchi,[7] S. Kasahara,[8] Y. Matsuda,[8] A. S. Sefat,[9] H. Ding,[2, 3, 4] P. Richard,[2, 3, 4, †] and G. Blumberg[1, 10, ‡]

[1]*Department of Physics and Astronomy, Rutgers University, Piscataway, NJ 08854, USA*
[2]*Beijing National Laboratory for Condensed Matter Physics,*
and Institute of Physics, Chinese Academy of Sciences, Beijing 100190, China
[3]*School of Physical Sciences, University of Chinese Academy of Sciences, Beijing 100190, China*
[4]*Collaborative Innovation Center of Quantum Matter, Beijing, China*
[5]*Center for Advanced Quantum Studies and Department of Physics,*
Beijing Normal University, Beijing 100875, China
[6]*Department of Physics and Astronomy, Rice University, Houston, Texas 77005, USA*
[7]*Department of Advanced Materials Science, University of Tokyo, Kashiwa, Chiba 277-8561, Japan*
[8]*Department of Physics, Kyoto University, Sakyo-ku, Kyoto 606-8502, Japan*
[9]*Materials Science & Technology Division, Oak Ridge National Laboratory, Oak Ridge, TN 37831*
[10]*National Institute of Chemical Physics and Biophysics, 12618 Tallinn, Estonia*
(Dated: December 7, 2017)

We used polarization-resolved Raman scattering to study the magneto-elastic coupling in the parent compounds of several families of Fe-based superconductors ($BaFe_2As_2$, $EuFe_2As_2$, $NaFeAs$, $LiFeAs$, $FeSe$ and $LaFeAsO$). We observe an emergent A_g-symmetry As phonon mode in the XY scattering geometry whose intensity is significantly enhanced below the magneto-structural transition only for compounds showing magnetic ordering. We conclude that the small lattice anisotropy is insufficient to induce the in-plane electronic polarizability anisotropy necessary for the observed phonon intensity enhancement, and interpret this enhancement below the Néel temperature in terms of the anisotropy of the magnetic moment and magneto-elastic coupling. We evidence a Fano line-shape in the XY scattering geometry resulting from a strong coupling between the A_g(As) phonon mode and the B_{2g} symmetry-like electronic continuum. Strong electron-phonon coupling may be relevant to superconductivity.

The lattice, orbital and magnetic degrees of freedom are strongly coupled in the Fe-based superconductors. This is best evidenced by the observation, in most parent compounds, of a magnetic transition from paramagnetic to collinear antiferromagnetic (AFM), occurring at a temperature T_N slightly lower than the temperature T_S at which a structural transition from tetragonal to orthorhombic phase occurs upon cooling. The interplay between these degrees of freedom is complex and led to a chicken-egg problem for which there is still no consensual view [1, 2]. The electronic structure is directly affected by the structural and magnetic transitions, notably through nematic transport properties [3–5], as well as by an electronic band folding accompanied by the formation of a spin-density-wave gap [6–9].

The As height and the related Fe-As-Fe angle are widely believed to play crucial roles in shaping the magnetic and electronic properties of the Fe-based superconductors [10–23]. Both parameters are modulated by the c-axis motion of the As atom corresponding to a fully symmetric phonon mode (A_{1g}) [24–30]. First-principles calculations show that the inclusion of the Fe spin ordering in the calculation of the As phonon mode frequency allows a good agreement with the energy of the As

phonon density-of-states measured by neutron scattering [31–37], suggesting significant magneto-elastic coupling.

Raman scattering can directly probe the As phonon behavior upon cooling across the magneto-structural transitions. As a signature of the magneto-elastic coupling, a finite intensity of the As phonon in nearly forbidden scattering geometries below the magneto-structural transition has been reported in $CaFe_2As_2$ [38], $EuFe_2As_2$ [39], $Ba(Fe_{1-x}Co_x)_2As_2$ [40–42], $Ba(Fe_{1-x}Au_x)_2As_2$ [43], $LaFeAsO$ [44]. In particular, the phonon shows an asymmetric line-shape below T_N in $Ba(Fe_{1-x}Co_x)_2As_2$, suggesting strong magneto-elastic coupling [40, 41]. However, the details behind this behavior, and its possible link to superconductivity, have not been stated satisfactorily. It has long been suggested that the electron-electron correlations enhance the electron-phonon coupling in the Fe-based superconductors and that the fully symmetric As vibration is related to the superconducting properties [22, 30, 45, 46].

In this Letter, we use polarized Raman scattering to study the temperature dependence of the magneto-elastic coupling for the fully symmetric phonon associated with the c-axis motion of the As atom for typical "122", "111", "1111" and "11" systems of Fe-based superconductors. For all compounds showing magnetic ordering, we observe strong intensity for the fully-symmetric As mode appearing below T_N in the nearly forbidden XY scattering channel as a result of significantly enhanced anisotropy of the in-plane electronic polarizabil-

TABLE I. Summary of T_S, T_N (in Kelvin), lattice orthorhombicity ($\delta = (a-b)/(a+b)$), intensity ratio of Ag phonon in XY and XX geometries, and ordered magnetic moment/Fe M (in μ_B) for compounds studied in this manuscript.

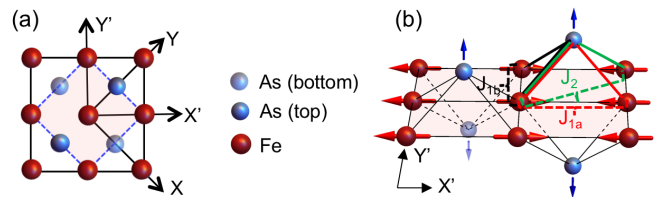| Sample	T_S/T_N	δ (%)	I_{XY}/I_{XX}	M
EuFe$_2$As$_2$ [47]	175/175	0.5 [54]	3.3	0.98 [55]
BaFe$_2$As$_2$ [47]	135/135	0.4 [56]	3.1	0.87 [57]
NaFeAs [49]	55/40	0.18 [58]	0.16	0.09 [57]
LaFeAsO [50, 51]	155/137	0.24 [59]	0.54	0.36-0.6 [57]
FeSe [52]	90/-	0.25 [60]	0.017	-
LiFeAs [61]	-/-	0	0	-

FIG. 1. (Color online) (a) Definition of the crystallographic directions in the tetragonal 2-Fe unit cell above T_S (light red shaded area) and 4-Fe orthorhombic magnetic unit cell below T_N (black solid lines). (b) Schematic diagram of the magnetic structure. Red arrows: Fe local moments forming collinear AFM order. Blue arrows: c-axes vibrations of the fully symmetric As phonon mode. The red and black solid lines illustrate the super-exchange paths of the nearest Fe neighbors, J_{1a} and J_{1b}. The green solid lines illustrate the super-exchange path of the next-nearest Fe neighbors, J_2.

ity, while no such enhancement is found for compounds without magnetically-ordered state. Because the lattice anisotropy $\delta = (a-b)/(a+b)$ below T_S is relatively small, we conclude that magneto-elastic coupling below T_N is essential. We interpret the A_g(As) phonon intensity enhancement below T_N in terms of strong coupling to the anisotropic in-plane magnetic moment. The study of the polarization dependence of the As phonon suggests that the mode is coupled to the non-symmetric XY-like electronic continuum. The asymmetric line-shape of A_g(As) phonon is described by a Fano model with a magneto-elastic coupling constant proportional to the magnetic order parameter. As the coupling between the XY-like electronic continuum and magnetism may survive in the superconducting compounds, our results emphasize the role played by the electron-phonon coupling in enhancing T_c.

Single crystals of materials listed in Table I were grown as described in Refs. [47–52]. The corresponding structural phase transition temperature (T_S) and magnetic phase transition temperature (T_N) are summarized in Table I. Raman measurements on BaFe$_2$As$_2$, NaFeAs, EuFe$_2$As$_2$, LiFeAs, FeSe were performed using the spectrometer described in Refs. [39, 53]. The measurements on LaFeAsO were performed in a back scattering geometry using a T64000 triple-stage spectrometer.

The phononic Raman scattering intensity is proportional to $I \propto |\hat{e}_i \cdot \mathbf{R} \cdot \hat{e}_s|^2$, where $\hat{e}_i$ and $\hat{e}_s$ are the polarization unit vectors of the incoming and scattering light, respectively, and $\mathbf{R}$ is the Raman tensor [62]. For the D_{4h} point group the XX, XY, $X'X'$ and $X'Y'$ polarization geometries probe $A_{1g} + B_{1g}$, $A_{2g} + B_{2g}$, $A_{1g} + B_{2g}$ and $A_{2g} + B_{1g}$ symmetry excitations, respectively. In the orthorhombic phase with D_{2h} point group symmetry, the unit cell rotates by 45°; the A_{1g} and B_{2g} representations of the D_{4h} point group merge into the A_g representation of the D_{2h} point group, and A_{2g} and B_{1g} (D_{4h}) merge into B_{1g} (D_{2h}). In the orthorhombic phase, the XX and XY polarization geometries probe $A_g + B_{1g}$ and A_g symmetry excitations, respectively [9].

Before investigating the behavior of the A_{1g}/A_g symmetry As phonon across the magneto-structural transi-

tions, we first examine the A_{1g} and A_g Raman tensors:

$$A_{1g}^{D_{4h}} = \begin{pmatrix} \bar{a} & 0 & 0 \\ 0 & \bar{a} & 0 \\ 0 & 0 & \bar{c} \end{pmatrix}, \quad A_g^{D_{2h}} = \begin{pmatrix} \frac{(\bar{a}'+\bar{b}')}{2} & \frac{(\bar{a}'-\bar{b}')}{2} & 0 \\ \frac{(\bar{a}'-\bar{b}')}{2} & \frac{(\bar{a}'+\bar{b}')}{2} & 0 \\ 0 & 0 & \bar{c} \end{pmatrix}$$

where $A_g^{D_{2h}}$ (orthorhombic phase) has been rotated by 45° to keep the same XYZ axis notation as in the tetragonal phase. $\bar{a}'$ and $\bar{b}'$ are the diagonal elements of the $A_g^{D_{2h}}$ Raman tensor in the natural coordinate system of the orthorhombic phase (before the 45° rotation).

Accordingly, the A_{1g}-symmetry mode is forbidden in the XY scattering geometry in the tetragonal phase. This is the case for LiFeAs, which shows no structural nor magnetic transition. As shown in Fig. 2(a), sharp Raman phonon peaks at 186 cm^{-1} and 237 cm^{-1}, corresponding to a A_{1g}(As) and a B_{1g}(Fe) modes, respectively, are detected in the XX scattering geometry. However, as expected for the tetragonal structure of LiFeAs, these modes have no intensity in the XY scattering geometry.

If anisotropy develops in the orthorhombic phase, the A_g anion mode may acquire a finite intensity $|(\bar{a}'-\bar{b}')/2|^2$ in the XY scattering geometry related to the anisotropy of the in-plane polarizability associated to this A_g anion mode because $\bar{a}'$ and $\bar{b}'$ are the polarizability derivatives along the two Fe-Fe orthogonal directions (X' and Y') in the orthorhombic phase. Since the lattice orthorhombicity δ is small (Table I), the intensity is expected to be weak. For example, for the FeSe material, which exhibits a structural transition at 90 K [63, 64] but no long-range magnetic ordering, we observe a A_g(Se) phonon at 180 cm^{-1} and a B_{1g}(Fe) phonon at 208 cm^{-1} for the XX polarization. Although the intensity of the A_g(Se) phonon with the XY polarization is finite at 20 K, it is only 2% of the corresponding intensity recorded for the XX polarization [Table I].

In contrast, BaFe$_2$As$_2$ with magnetic ordering clearly shows the 181 cm^{-1} A_g (As) mode [42, 65–67] in the XY scattering geometry below T_N [Fig. 2(c)]. Similar
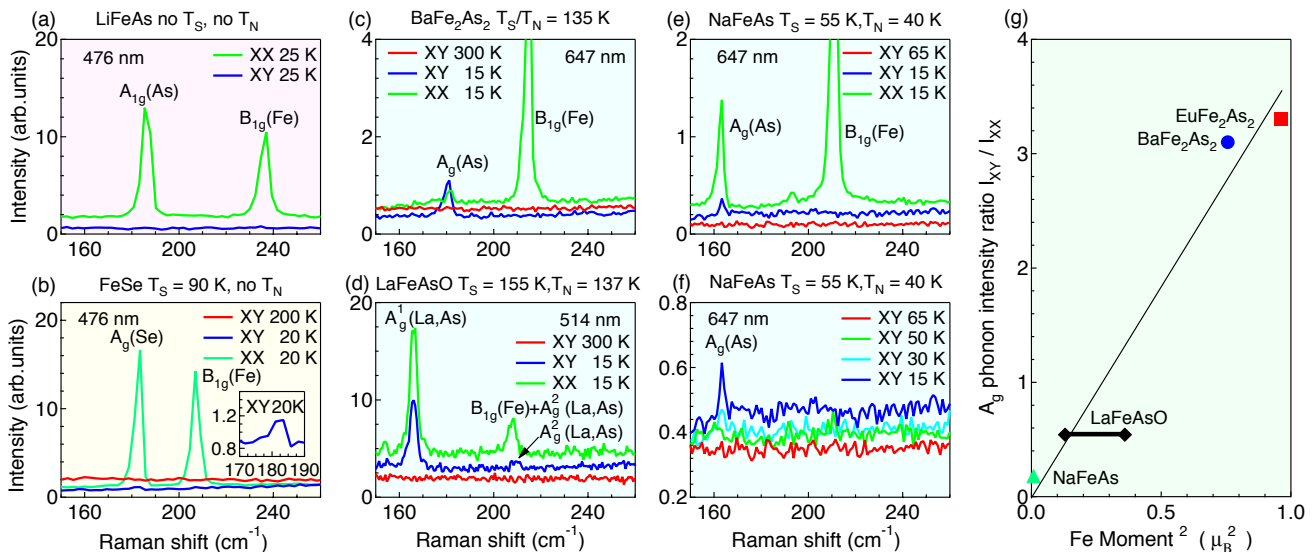
FIG. 2. Comparison of Raman spectra (shifted for clarity) for the XX and XY scattering geometries for different parent compounds: (a) LiFeAs, (b) FeSe, (c) BaFe$_2$As$_2$, (d) LaFeAsO, (e) and (f) NaFeAs. When finite, the T_N and T_S values are indicated on the top of the corresponding panel. (g) A_g(As) phonon intensity ratio in the XY and XX geometries (I_{XY}/I_{XX}) as a function of the squared ordered magnetic moment/Fe [55, 57]. The black line is a linear fit.

observation is made for NaFeAs [Figs. 2(e) and 2(f)], which also encounters both a structural and a magnetic transition: (i) We observe only a weak intensity between T_S and T_N, and (ii) the 162 cm^{-1} A_g(As) phonon mode appears in the XY spectra only below T_N. LaFeAsO [44, 68, 69] (Fig. 2(d)) is another system with split T_S and T_N transitions. In this case as well, we detect sizable intensity for the A_g^1(in-phase La and As) mode at 166 cm^{-1} and the A_g^2(out-of-phase La and As) mode at 209 cm^{-1} in the XY scattering geometry below T_N [Fig. 2(d)].

To quantify the intensity of the A_g(As) phonon in the XY scattering geometry below T_N in different families of Fe-based superconductors, we study the ratio between the A_g(As) peak intensity in the XY and XX scattering geometries I_{XY}/I_{XX}. This ratio is proportional to $|(\bar{a}' - \bar{b}')/(\bar{a}' + \bar{b}')|^2$, which is a direct measure of the in-plane polarizability anisotropy of the A_g(As) mode. Based on Table I, the ratio I_{XY}/I_{XX} is significant only for compounds with long-range magnetic ordering. For example, the ratio I_{XY}/I_{XX} is 300% for BaFe$_2$As$_2$, 16% for NaFeAs and 50% for LaFeAsO, as compared to 2% for FeSe, $i.$ $e.$ 1 to 2 orders of magnitude smaller. Such behavior cannot be solely explained by weak lattice orthorhombicity δ, and indicates that the intensity of the A_g(As) phonon in the XY scattering geometry is mainly controlled by the magneto-elastic coupling, for which we argue that the strength originates from the anisotropy of the magnetic interactions in the Fe-As plane that are modulated by the c-axis motion of the As atoms. We can estimate the strength of the magneto-elastic coupling by comparing the I_{XY}/I_{XX} intensity ratios in the

magnetically-ordered compounds to that in FeSe. As compared to FeSe, the coupling strength values are 200, 25 and 8 in BaFe$_2$As$_2$, LaFeAsO and NaFeAs, respectively.

In Fig. 2(g), we show that the I_{XY}/I_{XX} ratio of the A_g(As) phonon intensity for different Fe-based materials scales linearly with the square of the magnetic moment M, indicating that the magneto-elastic coupling constant is proportional to the ordered magnetic moment M. In Ref. [23], the magneto-elastic coupling was explicitly calculated within a tight-binding Slater-Koster formalism. The study predicts a large enhancement of the As mode in the XY scattering geometry, consistent with experimental observation [Fig. 2], due to the anisotropy of the Slater-Koster energy integrals in the magnetically ordered state.

Above we have established that the intensity enhancement of the A_g(As) phonon mode in the XY scattering geometry depends on the presence of ordered magnetic moment. We now address the coupling between the A_g(As) phonon and the B_{2g}-like electronic continuum below T_N. In Figs. 3(a-b) we present the polarization dependence of the spectra for BaFe$_2$As$_2$ and EuFe$_2$As$_2$ at 15 K. The line-shape of the A_g(As) phonon in the XX and ZZ scattering geometries is symmetric, in contrast to asymmetric interference Fano shape observed in the XY and $X'X'$ geometries [62, 70]. The polarization analysis suggests that interfering with the phonon electronic continuum must have B_{2g} symmetry. A B_{2g}-like continuum is allowed to couple to A_g(As) phonon in the orthorhombic phase because below the $D_{4h} \rightarrow D_{2h}$ transition the A_{1g} and B_{2g} representations merge into the
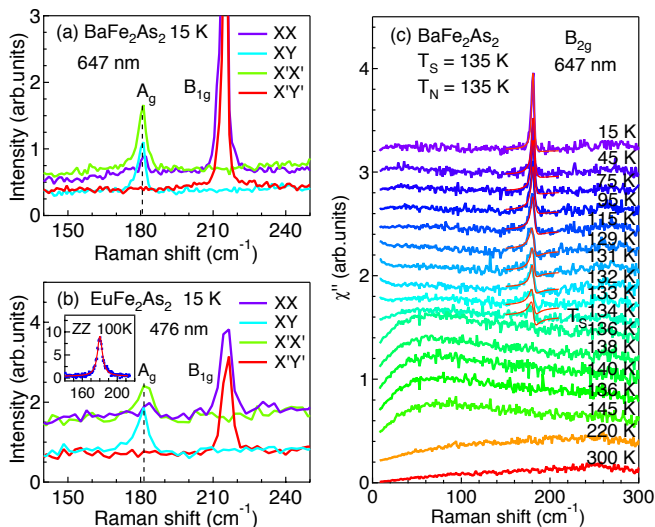
4

FIG. 3. (Color online) Raman spectra in the XX, XY, $X'X'$ and $X'Y'$ geometries for (a) $BaFe_2As_2$ and (b) $EuFe_2As_2$ at 15 K. The inset in (b) shows spectra for ZZ polarization from a polished ac surface of $EuFe_2As_2$ for the in the magnetic state at 100 K excited with 752 nm laser line [72]. The red line is a fit of the A_g phonon with a Lorentzian function. (c) T-dependence of Raman spectra for $BaFe_2As_2$ in the XY scattering geometry (shifted for clarity). The solid red lines are Fano-shape fits [43]. The spectral resolution is about $0.85\,cm^{-1}$.

A_g irreducible representation. For XY and $X'X'$ geometry, where the B_{2g}-like continuum is represent, the bare $A_g(As)$ phonon is coupled to the B_{2g}-like electronic continuum, giving rise to an asymmetric Fano line-shape.

In addition, we argue that the density-of-states of the B_{2g}-like continuum is temperature-dependent. In Fig. 3(c), we show temperature evolution of the Raman spectra in XY scattering geometry for $BaFe_2As_2$. Just below T_N the $A_g(As)$ phonon instantly appears with a visibly asymmetric line-shape. The mode sharpens and becomes more symmetric upon cooling, which we attribute to a decrease in the electronic density-of-states at the Fermi level, contributing to the B_{2g}-like continuum, due to the spin-density-wave gap formation [6–9].

To quantify the electron-phonon interaction, we constructed a Fano model (Eq. 3 in Ref. [43]) with a magneto-elastic coupling constant proportional to the magnetic ordered moment. The Fano interference is between the $A_g(As)$ phonon mode and the B_{2g}-like electronic continuum below T_N. Such model well describes

the data for $BaFe_2As_2$, Fig. 3(c). Same approach also describes all spectral features for $Ba(Fe_{1-x}Au_x)_2As_2$ [43]. Hence, the polarization-resolved Raman spectroscopy implemented here represents an all-inclusive tool to study the magnetism and the magneto-elastic interaction in the Fe-based superconductors.

Finally, we discuss the implications of the electron-phonon coupling to superconductivity. Early calculations show that when magnetic moments are included [73], the electron-phonon coupling is enhanced by 50% as compared with non-magnetic calculations [74]. According to more recent calculations, the electron-phonon matrix element is rather enhanced four times in the ordered AFM state due to the presence of a d_{xz}/d_{yz} Fermi surface near the zone corner [75, 76]. In particular, the Eliashberg spectral function α^2F is enhanced 4 times around 22 meV, which corresponds to the A_{1g} mode energy [75, 76]. Thus, one cannot rule out the possibility that the enhanced intraband electron-phonon coupling in the AFM phase, if sufficiently large, could enhance the paring temperature.

In conclusion, we revealed a significant intensity enhancement of the emergent $A_g(As)$ phonon mode in the XY scattering geometry below T_N only for parent compounds of Fe-based superconductors showing magnetic order. We argue that the in-plane electronic polarizability anisotropy necessary for the $A_g(As)$ phonon intensity enhancement originates from the anisotropy of the magnetic interactions in the Fe-As plane that are modulated by the c-axis motion of the As atoms. In particular, we demonstrate a magneto-elastic coupling between the $A_g(As)$ phonon and the B_{2g}-like electronic continuum that is essential to $A_g(As)$ phonon intensity enhancement. The asymmetric line-shape of $A_g(As)$ phonon is well explained by a Fano model with a magneto-elastic coupling constant proportional to the ordered magnetic moment. Our results identify strong electron-phonon coupling in the magnetic phase of Fe-based superconductors, which could enhance the paring temperature.

[1] R. M. Fernandes, A. V. Chubukov, and J. Schmalian, "What drives nematic order in iron-based superconductors?" Nat. Phys. 10, 97 (2014).

[2] R. M. Fernandes, L. H. VanBebber, S. Bhattacharya, P. Chandra, V. Keppens, D. Mandrus, M. A. McGuire, B. C. Sales, A. S. Sefat, and J. Schmalian, "Effects of nematic fluctuations on the elastic properties of iron arsenide superconductors," Phys. Rev. Lett. 105, 157003 (2010).

[3] J.-H. Chu, J. G. Analytis, K. De Greve, P. L. McMa-

hon, Z. Islam, Y. Yamamoto, and I. R. Fisher, "In-plane resistivity anisotropy in an underdoped iron arsenide superconductor," Science **329**, 824 (2010).

[4] J. H. Chu, H. H. Kuo, J. G. Analytis, and I. R. Fisher, "Divergent nematic susceptibility in an iron arsenide superconductor," Science **337**, 710 (2012).

[5] H. H. Kuo, J. H. Chu, J. C. Palmstrom, S. A. Kivelson, and I. R. Fisher, "Ubiquitous signatures of nematic quantum criticality in optimally doped Fe-based superconductors," Science **352**, 958 (2016).

[6] W. Z. Hu, J. Dong, G. Li, Z. Li, P. Zheng, G. F. Chen, J. L. Luo, and N. L. Wang, "Origin of the spin density wave instability in AFe_2As_2 (A=Ba,Sr) as revealed by optical spectroscopy," Phys. Rev. Lett. **101**, 257005 (2008).

[7] Y. Ran, F. Wang, H. Zhai, A. Vishwanath and D.-H. Lee, "Nodal spin density wave and band topology of the FeAs-based materials," Phys. Rev. B **79**, 014505 (2009).

[8] P. Richard, K. Nakayama, T. Sato, M. Neupane, Y.-M. Xu, J. H. Bowen, G. F. Chen, J. L. Luo, N. L. Wang, X. Dai, Z. Fang, H. Ding and T. Takahashi, "Observation of Dirac Cone Electronic Dispersion in $BaFe_2As_2$," Phys. Rev. Lett. **104**, 137001 (2010).

[9] W.-L. Zhang, Z. P. Yin, A. Ignatov, Z. Bukowski, Janusz Karpinski, Athena S. Sefat, H. Ding, P. Richard, and G. Blumberg, "Raman scattering study of spin-density-wave-induced anisotropic electronic properties in AFe_2As_2 (A=Ca, Eu)," Phys. Rev. B **93**, 205106 (2016).

[10] K. Kuroki, H. Usui, S. Onari, R. Arita, and H. Aoki, "Pnictogen height as a possible switch between high-T_c nodeless and low-T_c nodal pairings in the iron-based superconductors," Phys. Rev. B **79**, 224511 (2009).

[11] J. D. Lee, W. S. Yun, and S. C. Hong, "Ultrafast above-transition-temperature resurrection of spin density wave driven by coherent phonon generation in $BaFe_2As_2$," New J. Phys. **16**, 043010 (2014).

[12] V. Balédent, F. Rullier-Albenque, D. Colson, J. M. Ablett, and J.-P. Rueff, "Electronic properties of $BaFe_2As_2$ upon doping and pressure: The prominent role of the As p orbitals," Phys. Rev. Lett. **114**, 177001 (2015).

[13] V. Vildosola, L. Pourovskii, R. Arita, S. Biermann, and A. Georges, "Bandwidth and Fermi surface of iron oxypnictides: Covalency and sensitivity to structural changes," Phys. Rev. B **78**, 064518 (2008).

[14] M. J. Calderón, B. Valenzuela, and E. Bascones, "Tight-binding model for iron pnictides," Phys. Rev. B **80**, 094531 (2009).

[15] Z. P. Yin, S. Lebègue, M. J. Han, B. P. Neal, S. Y. Savrasov, and W. E. Pickett, "Electron-hole symmetry and magnetic coupling in antiferromagnetic LaFeAsO," Phys. Rev. Lett. **101**, 047001 (2008).

[16] F. Yndurain, "Coupling of magnetic moments with phonons and electron-phonon interaction in $LaFeAsO_{1-x}F_x$," EPL **94**, 37001 (2011).

[17] C. de la Cruz, W. Z. Hu, S. L Li, Q. Huang, J. W. Lynn, M. A. Green, G. F. Chen, N. L. Wang, H. A. Mook, Q. M Si, and P. C Dai, "Lattice distortion and magnetic quantum phase transition in $CeFeAs_{1-x}P_xO$," Phys. Rev. Lett. **104**, 017204 (2010).

[18] C. L. Zhang, L. W. Harriger, Z. P. Yin, W. C. Lv, M. Y. Wang, G. T. Tan, Y. Song, D. L. Abernathy, W. Tian, T. Egami, K. Haule, G. Kotliar, and P. C. Dai, "Effect of pnictogen height on spin waves in iron pnictides," Phys.
Rev. Lett. **112**, 217202 (2014).

[19] C. H Lee, A. Iyo, H. Eisaki, H. Kito, M. T. Fernandez-Diaz, T. Ito, K. Kihou, H. Matsuhata, M. Braden, and K. Yamada, "Effect of structural parameters on superconductivity in fluorine-free $LnFeAsO_{1-y}$ (Ln = La, Nd)," J. Phys. Soc. Jpn. **77**, 083704 (2008).

[20] J. Zhao, Q. Huang, C. de la Cruz, S. L. Li, J. W. Lynn, Y. Chen, M. A. Green, G. F. Chen, G. Li, Z. Li, J. L. Luo, N. L. Wang, and P. C. Dai, "Structural and magnetic phase diagram of $CeFeAsO_{1-x}F_x$ and its relation to high-temperature superconductivity," Nat. Mater. **7**, 953–959 (2008).

[21] K. Kuroki, H. Usui, S. Onari, R. Arita, and H. Aoki, "Pnictogen height as a possible switch between high-T_c nodeless and low-T_c nodal pairings in the iron-based superconductors," Phys. Rev. B **79**, 224511 (2009).

[22] G. Garbarino, R. Weht, A.Sow, C. Lacroix, A. Sulpice, M. Mezouar, X. Zhu, F. Han, H. H. Wen, and M. Nez-Regueiro, "Direct observation of the influence of the $FeAs_4$ tetrahedron on superconductivity and antiferromagnetic correlations in Sr_2VO_3FeAs," EPL **96**, 57002 (2011).

[23] N. A. García-Martínez, B. Valenzuela, S. Ciuchi, E. Cappelluti, M. J. Calderón, and E. Bascones, "Coupling of the As A_{1g} phonon to magnetism in iron pnictides," Phys. Rev. B **88**, 165106 (2013).

[24] B. Mansart, D. Boschetto, A. Savoia, F. Rullier-Albenque, A. Forget, D. Colson, A. Rousse, and M. Marsi, "Observation of a coherent optical phonon in the iron pnictide superconductor $Ba(Fe_{1-x}Co_x)_2As_2$ ($x = 0.06$ and 0.08)," Phys. Rev. B **80**, 172504 (2009).

[25] K. W. Kim, A. Pashkin, H. Schäfer, M. Beyer, M. Porer, T. Wolf, C. Bernhard, J. Demsar, R. Huber, and A. Leitenstorfer, "Ultrafast transient generation of spin-density-wave order in the normal state of $BaFe_2As_2$ driven by coherent lattice vibrations," Nat. Mater. **11**, 497–501 (2012).

[26] I. Avigo, R. Corts, L. Rettig, S. Thirupathaiah, H. S. Jeevan, P. Gegenwart, T. Wolf, M. Ligges, M. Wolf, J. Fink, and U. Bovensiepen, "Coherent excitations and electronphonon coupling in $Ba/EuFe_2As_2$ compounds investigated by femtosecond time- and angle-resolved photoemission spectroscopy," J. Phys.: Condens. Matter **25**, 094003 (2013).

[27] L. X. Yang, G. Rohde, T. Rohwer, A. Stange, K. Hanff, C. Sohrt, L. Rettig, R. Cortés, F. Chen, D. L. Feng, T. Wolf, B. Kamble, I. Eremin, T. Popmintchev, M. M. Murnane, H. C. Kapteyn, L. Kipp, J. Fink, M. Bauer, U. Bovensiepen, and K. Rossnagel, "Ultrafast modulation of the chemical potential in $BaFe_2As_2$ by coherent phonons," Phys. Rev. Lett. **112**, 207001 (2014).

[28] S. Gerber, K. W. Kim, Y. Zhang, D. Zhu, N. Plonka, M. Yi, G. L. Dakovski, D. Leuenberger, P. S. Kirchmann, R. G. Moore, M. Chollet, J. M. Glownia, Y. Feng, J.-S. Lee, A. Mehta, A. F. Kemper, T. Wolf, Y.-D. Chuang, Z. Hussain, C.-C. Kao, B. Moritz, Z.-X. Shen, T. P. Devereaux, and W.-S. Lee, "Direct characterization of photoinduced lattice dynamics in $BaFe_2As_2$," Nat. Commun. **6**, 7377 (2015).

[29] L. Rettig, S. O. Mariager, A. Ferrer, S. Grübel, J. A. Johnson, J. Rittmann, T. Wolf, S. L. Johnson, G. Ingold, P. Beaud, and U. Staub, "Ultrafast structural dynamics of the Fe-pnictide parent compound $BaFe_2As_2$," Phys. Rev. Lett. **114**, 067402 (2015).

[30] S. Mandal, R. E. Cohen, and K. Haule, "Strong pressure-dependent electron-phonon coupling in FeSe," Phys. Rev. B **89**, 220502 (2014).

[31] T. Yildirim, "Frustrated magnetic interactions, giant magnetoelastic coupling, and magnetic phonons in iron pnictides," Physica C **469**, 425 (2009).

[32] L. Boeri, M. Calandra, I. I. Mazin, O. V. Dolgov, and F. Mauri, "Effects of magnetism and doping on the electron-phonon coupling in $BaFe_2As_2$," Phys. Rev. B **82**, 020506 (2010).

[33] M. Zbiri, H. Schober, M. R. Johnson, S. Rols, R. Mittal, Y. X. Su, M. Rotter, and D. Johrendt, "*ab* initio lattice dynamics simulations and inelastic neutron scattering spectra for studying phonons in $BaFe_2As_2$: Effect of structural phase transition, structural relaxation, and magnetic ordering," Phys. Rev. B **79**, 064511 (2009).

[34] D. Reznik, K. Lokshin, D. C. Mitchell, D. Parshall, W. Dmowski, D. Lamago, R. Heid, K.-P. Bohnen, A. S. Sefat, M. A. McGuire, B. C. Sales, D. G. Mandrus, A. Subedi, D. J. Singh, A. Alatas, M. H. Upton, A. H. Said, A. Cunsolo, Yu. Shvyd'ko, and T. Egami, "Phonons in doped and undoped $BaFe_2As_2$ investigated by inelastic x-ray scattering," Phys. Rev. B **80**, 214534 (2009).

[35] S. E. Hahn, Y. Lee, N. Ni, P. C. Canfield, A. I. Goldman, R. J. McQueeney, B. N. Harmon, A. Alatas, B. M. Leu, E. E. Alp, D. Y. Chung, I. S. Todorov, and M. G. Kanatzidis, "Influence of magnetism on phonons in $CaFe_2As_2$ as seen via inelastic x-ray scattering," Phys. Rev. B **79**, 220511 (2009).

[36] R. Mittal, M. K. Gupta, S. L. Chaplot, M. Zbiri, S. Rols, H. Schober, Y. Su, Th. Brueckel, and T. Wolf, "Spin-phonon coupling in $K_{0.8}Fe_{1.6}Se_2$ and KFe_2Se_2: Inelastic neutron scattering and *ab* initio phonon calculations," Phys. Rev. B **87**, 184502 (2013).

[37] S. E. Hahn, G. S. Tucker, J.-Q. Yan, A. H. Said, B. M. Leu, R. W. McCallum, E. E. Alp, T. A. Lograsso, R. J. McQueeney, and B. N. Harmon, "Magnetism-dependent phonon anomaly in LaFeAsO observed via inelastic x-ray scattering," Phys. Rev. B **87**, 104518 (2013).

[38] K. Y. Choi, D. Wulferding, P. Lemmens, N. Ni, S. L. Bud'ko, and P. C. Canfield, "Lattice and electronic anomalies of $CaFe_2As_2$ studied by Raman spectroscopy," Phys. Rev. B **78**, 212503 (2008).

[39] W. L. Zhang, P. Richard, H. Ding, A. S. Sefat, J. Gillett, S. E. Sebastian, M. Khodas, and G. Blumberg, "On the origin of the electronic anisotropy in iron pnicitde superconductors," arXiv:1410.6452 (2014).

[40] L. Chauvière, Y. Gallais, M. Cazayous, M. A. Méasson, A. Sacuto, D. Colson, and A. Forget, "Raman scattering study of spin-density-wave order and electron-phonon coupling in $Ba(Fe_{1-x}Co_x)_2As_2$," Phys. Rev. B **84**, 104508 (2011).

[41] F. Kretzschmar, T. Bohm, U. Karahasanovic, B. Muschler, A. Baum, D. Jost, J. Schmalian, S. Caprara, M. Grilli, C. Di Castro, J. G. Analytis, J.-H. Chu, I. R. Fisher, and R. Hackl, "Critical spin fluctuations and the origin of nematic order in $Ba(Fe_{1-x}Co_x)_2As_2$," Nat. Phys. **12**, 560 (2016).

[42] S. Sugai, Y. Mizuno, R. Watanabe, T. Kawaguchi, K. Takenaka, H. Ikuta, Y. Takayanagi, N. Hayamizu, and Y. Sone, "Spin-density-wave gap with Dirac nodes and two-magnon raman scattering in $BaFe_2As_2$," J. Phys. Soc. Jpn. **81**, 024718 (2012).

[43] S.-F. Wu, W.-L. Zhang, L. Li, H. B. Cao, Sefat A. S. Kung, H.-H., H. Ding, P. Richard, and G. Blumberg, "Anomalous magneto-elastic coupling in Au-doped $BaFe_2As_2$," Submitted to PRB.

[44] U. F. Kaneko, P. F. Gomes, A. F. Garcia-Flores, J. Q. Yan, T. A. Lograsso, G. E. Barberis, D. Vaknin, and E. Granado, "Nematic fluctuations and phase transitions in LaFeAsO: a Raman scattering study," Phys. Rev. B **96**, 257005 (2008).

[45] T. Egami, B. V. Fine, D. Parshall, A. Subedi, and D. J. Singh, "Spin-lattice coupling and superconductivity in Fe pnictides," J. Adv. Cond. Matter Phys. **7**, 164916 (2010).

[46] S. Gerber, S.-L. Yang, D. Zhu, H. Soifer, J. A. Sobota, S. Rebec, J. J. Lee, T. Jia, B. Moritz, C. Jia, A. Gauthier, Y. Li, D. Leuenberger, Y. Zhang, L. Chaix, W. Li, H. Jang, J.-S. Lee, M. Yi, G. L. Dakovski, S. Song, J. M. Glownia, S. Nelson, K. W. Kim, Y.-D. Chuang, Z. Hussain, R. G. Moore, T. P. Devereaux, W.-S. Lee, P. S. Kirchmann, and Z.-X. Shen, "Femtosecond electron-phonon lock-in by photoemission and x-ray free-electron laser," Science **357**, 71 (2017).

[47] A. S. Sefat, "Bulk synthesis of iron-based superconductors," Curr. Opin. Solid State Mater. Sci. **17**, 59–64 (2013).

[48] L. Li, H. B. Cao, M. A. McGuire, J. S. Kim, G. R. Stewart, and A. S. Sefat, "Role of magnetism in superconductivity of $BaFe_2As_2$: Study of 5*d* Au-doped crystals," Phys. Rev. B **92**, 094504 (2015).

[49] M. A. Tanatar, N. Spyrison, Kyuil Cho, E. C. Blomberg, Guotai Tan, Pengcheng Dai, Chenglin Zhang, and R. Prozorov, "Evolution of normal and superconducting properties of single crystals of $Na_{1-\delta}FeAs$ upon interaction with environment," Phys. Rev. B **85**, 014510 (2012).

[50] Y. Kamihara, T. Watanabe, M. Hirano, and H. Hosono, "Iron-based layered superconductor $LaO_{1-x}F_xFeAs$ (x = $0.05 - 0.12$) with T_c = 26 K," J. Am. Chem. Soc **130**, 3296 (2008).

[51] C. de la Cruz, Q. Huang, J. W. Lynn, Jiying Li, W. Ratcliff II, J. L. Zarestky, H. A. Mook, G. F. Chen, J. L. Luo, N. L. Wang, and P. C Dai, "Magnetic order close to superconductivity in the iron-based layered $LaO_{1-x}F_xFeAs$ systems," Nature **453**, 899 (2008).

[52] S. Hosoi, K. Matsuura, K. Ishida, H. Wang, Y. Mizukami, T. Watashige, S. Kasahara, Y. Matsuda, and T. Shibauchi, "Nematic quantum critical point without magnetism in $FeSe_{1-x}S_x$ superconductors," Proc. Natl. Acad. Sci. U.S.A. **113**, 8139 (2016).

[53] V. K. Thorsmølle, M. Khodas, Z. P. Yin, Chenglin Zhang, S. V. Carr, Pengcheng Dai, and G. Blumberg, "Critical quadrupole fluctuations and collective modes in iron pnictide superconductors," Phys. Rev. B **93**, 054515 (2016).

[54] M. Tegel, M. Rotter, V. Wei, F. M. Schappacher, R. Pttgen, and D. Johrendt, "Structural and magnetic phase transitions in the ternary iron arsenides $SrFe_2As_2$ and $EuFe_2As_2$," J. Phys.: Condens. Matter **20**, 452201 (2008).

[55] Y. Xiao, Y. Su, M. Meven, R. Mittal, C. M. N. Kumar, T. Chatterji, S. Price, J. Persson, N. Kumar, S. K. Dhar, A. Thamizhavel, and Th. Brueckel, "Magnetic structure of $EuFe_2As_2$ determined by single-crystal neutron diffraction," Phys. Rev. B **80**, 174424 (2009).

[56] Q. Huang, Y. Qiu, Wei Bao, M. A. Green, J. W. Lynn, Y. C. Gasparovic, T. Wu, G. Wu, and X. H.

Chen, "Neutron-diffraction measurements of magnetic order and a structural transition in the parent $BaFe_2As_2$ compound of FeAs-based high-temperature superconductors," Phys. Rev. Lett. **101**, 257003 (2008).

[57] P. C. Dai, "Antiferromagnetic order and spin dynamics in iron-based superconductors," Rev. Mod. Phys. **87**, 855 (2015).

[58] S. L Li, C. de la Cruz, Q. Huang, G. F. Chen, T.-L. Xia, J. L. Luo, N. L. Wang, and P. C Dai, "Structural and magnetic phase transitions in $Na_{1-\delta}FeAs$," Phys. Rev. B **80**, 020504 (2009).

[59] C. de la Cruz, Q. Huang, J. W. Lynn, J.Y. Li, W. R. II, J. L. Zarestky, H. A. Mook, G. F. Chen, J. L. Luo, N. L. Wang, and P. C Dai, "Magnetic order close to superconductivity in the iron-based layered $LaO_{1-x}F_xFeAs$ systems," Nature **453**, 899 (2008).

[60] T. M. McQueen, A. J. Williams, P. W. Stephens, J. Tao, Y. Zhu, V. Ksenofontov, F. Casper, C. Felser, and R. J. Cava, "Tetragonal-to-orthorhombic structural phase transition at 90 K in the superconductor $Fe_{1.01}Se$," Phys. Rev. Lett. **103**, 057002 (2009).

[61] X. C. Wang, Q. Q. Liu, Y. X. Lv, Z. Deng, K. Zhao, R. C. Yu, J. L. Zhu, and C. Q Jin, "Superconducting properties of "111" type LiFeAs iron arsenide single crystals," Sci. China Phys. Mech. **53**, 1199 (2010).

[62] K. Cardona, "Light scattering in solids I, Introductory Concepts," Topics in Applied Physics **8** (1983).

[63] A. E. Böhmer, F. Hardy, F. Eilers, D. Ernst, P. Adelmann, P. Schweiss, T. Wolf, and C. Meingast, "Lack of coupling between superconductivity and orthorhombic distortion in stoichiometric single-crystalline FeSe," Phys. Rev. B **87**, 180505(R) (2013).

[64] A. E. Böhmer, T. Arai, F. Hardy, T. Hattori, T. Iye, T. Wolf, H. v Loehneysen, K. Ishida, and C. Meingast, "Origin of the Tetragonal-to-Orthorhombic Phase Transition in FeSe: A Combined Thermodynamic and NMR Study of Nematicity," Phys. Rev. Lett. **114**, 027001 (2015).

[65] A. P. Litvinchuk, V. G. Hadjiev, M. N. Iliev, Bing Lv, A. M. Guloy, and C. W. Chu, "Raman-scattering study of $K_xSr_{1-x}Fe_2As_2$($x =0.0,0.4$)," Phys. Rev. B **78**, 060503 (2008).

[66] L. Chauvière, Y. Gallais, M. Cazayous, A. Sacuto, M. A. Méasson, D. Colson, and A. Forget, "Doping dependence of the lattice dynamics in $Ba(Fe_{1-x}Co_x)_2As_2$ studied by Raman spectroscopy," Phys. Rev. B **80**, 094504 (2009).

[67] M. Rahlenbeck, G. L. Sun, D. L. Sun, C. T. Lin, B. Keimer, and C. Ulrich, "Phonon anomalies in pure and underdoped $R_{1-x}K_xFe_2As_2$ (R=Ba, Sr) investigated by raman light scattering," Phys. Rev. B **80**, 064509 (2009).

[68] V. G. Hadjiev, M. N. Iliev, K. Sasmal, Y.-Y. Sun, and C. W. Chu, "Raman spectroscopy of RFeAsO(R=Sm, La)," Phys. Rev. B **77**, 220505 (2008).

[69] S. C. Zhao, D. Hou, Y. Wu, T. L. Xia, A. M. Zhang, G. F. Chen, J. L. Luo, N. L. Wang, J. H. Wei, Z. Y. Lu, and Q. M. Zhang, "Raman spectra in iron-based quaternary $CeO_{1-x}F_xFeAs$ and $LaO_{1-x}F_xFeAs$," Supercond. Sci. Technol. **22**, 015017 (2009).

[70] U. Fano, "Effects of configuration interaction on intensities and phase shifts," Phys. Rev. **124**, 1866 (1961).

[71] As a result of the sum rule, what we observe in the $X'X'$ scattering geometry is the sum of the bare mode and the Fano interference.

[72] W.-L. Zhang, Athena S. Sefat, H. Ding, P. Richard, and G. Blumberg, "Stress-induced nematicity in $EuFe_2As_2$ studied by Raman spectroscopy," Phys. Rev. B **94**, 014513 (2016).

[73] L. Boeri, M. Calandra, I. I. Mazin, O. V. Dolgov, and F. Mauri, "Effects of magnetism and doping on the electron-phonon coupling in $BaFe_2As_2$," Phys. Rev. B **82**, 020506 (2010).

[74] L. Boeri, O. V. Dolgov, and A. A. Golubov, "Is $LaFeAsO_{1-x}F_x$ an electron-phonon superconductor?" Phys. Rev. Lett. **101**, 026403 (2008).

[75] S. Coh, M. L. Cohen, and S. G. Louie, "Antiferromagnetism enables electron-phonon coupling in iron-based superconductors," Phys. Rev. B **94**, 104505 (2016).

[76] S. Coh, M. L. Cohen, and S. G. Louie, "Large electron-phonon interactions from FeSe phonons in a monolayer," New J. Phys. **17**, 073027 (2015).